Supplementary Material

Title: CdS@Ni_3S_2 core-shell nanorod arrays on nickel foam: a multifunctional catalyst for efficient electrochemical catalytic, photoelectrochemical and photocatalytic H_2 production reaction

HaojianGuan,[a] ShengsenZhang,[a] Xin Cai,[a] QiongzhiGao,[a] XiaoyuanYu,[a]

XiaosongZhou,[c] Feng Peng,*[b] Yueping Fang,*[a] Siyuan Yang*[a]

[a] College of Materials and Energy, South China Agricultural University, Guangzhou, 510642, Peoples' Republic of China

*E-mail: siyuan_yang@scau.edu.cn; ypfang@scau.edu.cn

[b] School of Chemistry and Chemical Engineering, Guangzhou University, Guangzhou, 510006, Peoples' Republic of China

*E-mail:fpeng@gzhu.edu.cn

[c] School of Chemistry and Chemical Engineering, and Institute of Physical Chemistry, Lingnan Normal University, Zhanjiang, 524048, Peoples' Republic of China

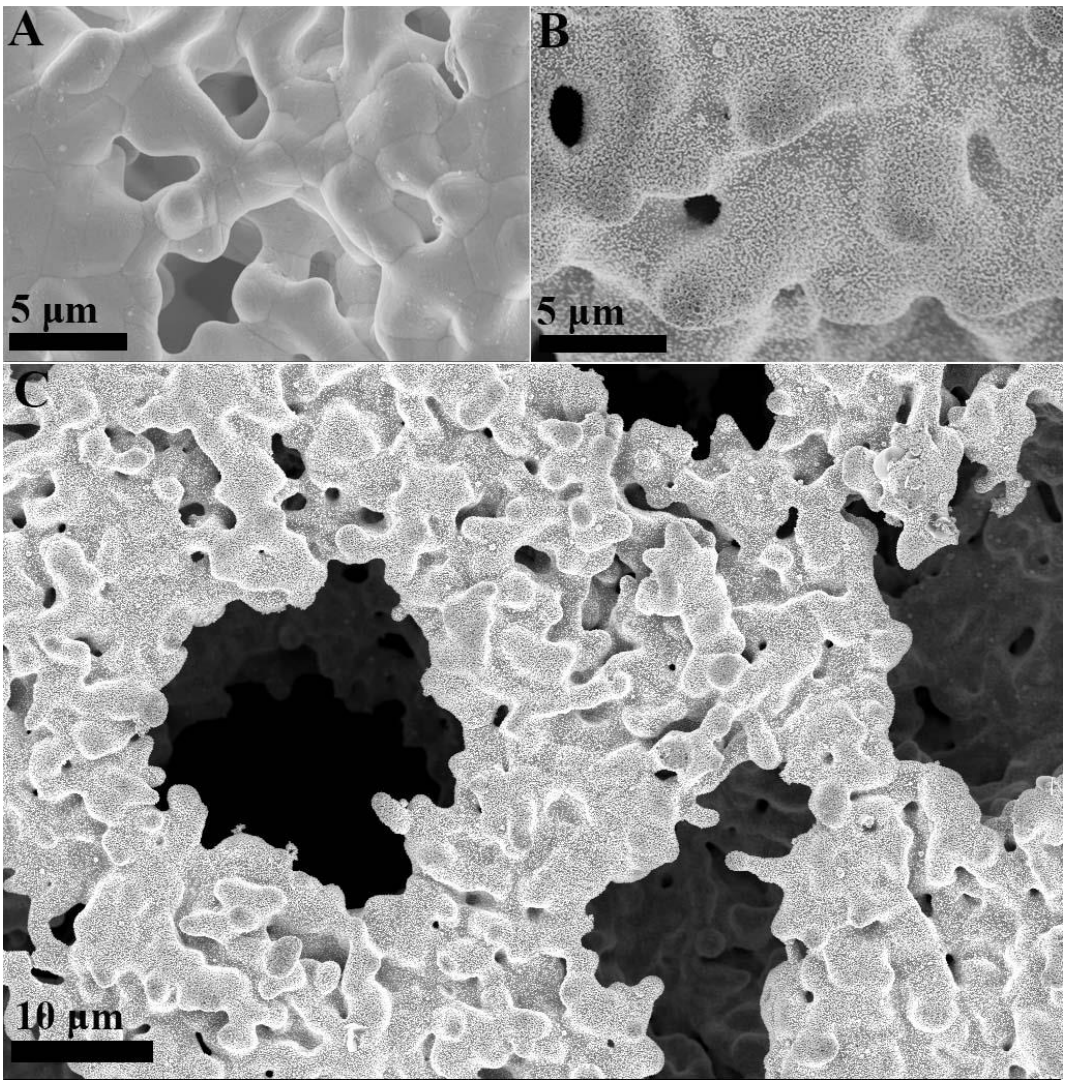

Fig. S1. Low magnification SEM images of: (A) pure Ni foam and (B) CdS@Ni_3S_2core@shell nanorods arrays on Ni foam after the hydrothermal synthesized process; (C) A large-scale SEM image of the typical CdS@Ni_3S_2 nanorod arrays on the Ni foam, which demonstrated the homogeneous of the sample.

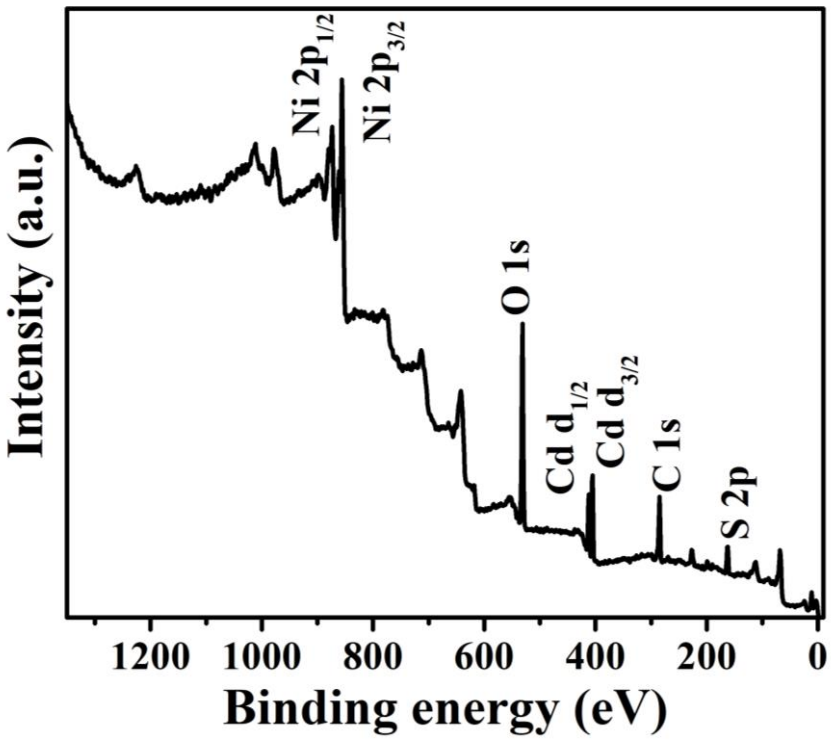

Fig. S2. The XPS survey spectrum of a typical CdS@Ni_3S_2 samples.

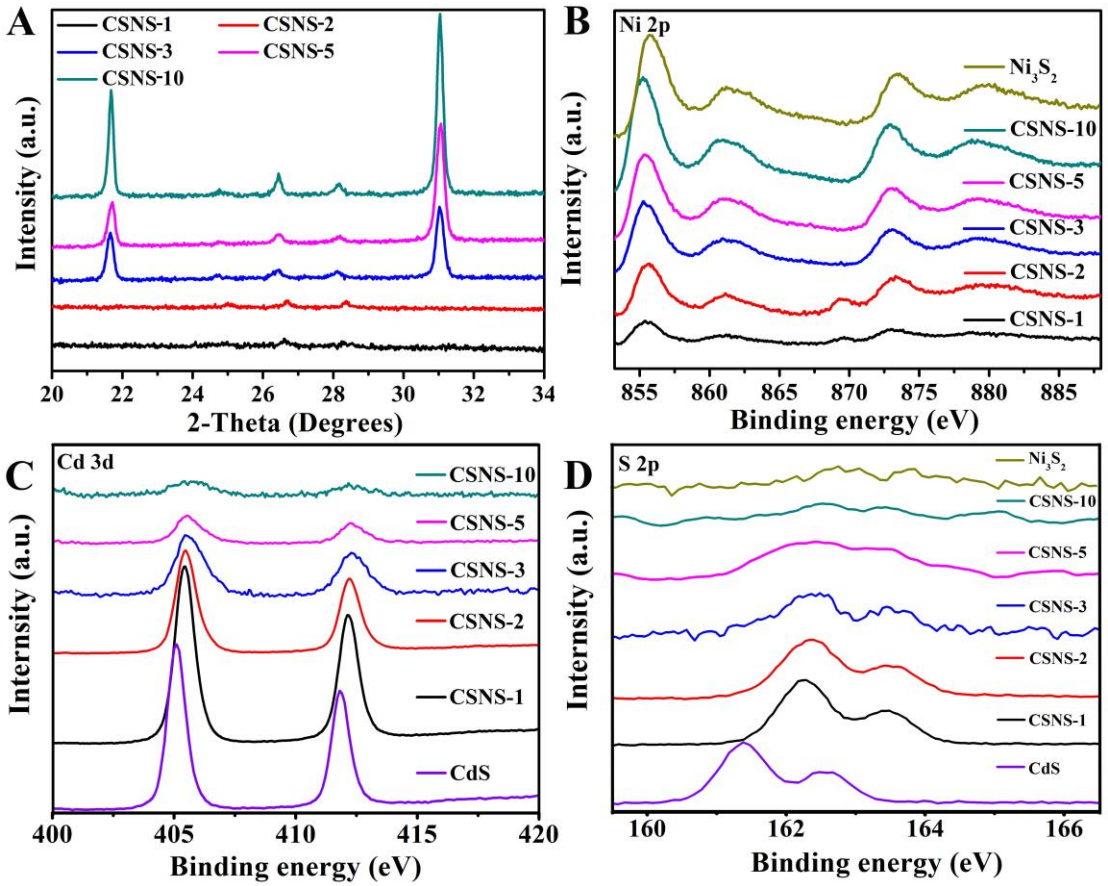

Fig. S3. XRD (A) and high-resolution XPS spectra of the CSNS-x samples, pure CdS and pure Ni_3S_2 samples with Ni 2p (B), Cd 3d (C) and S 2p (D) spectrum.

As shown in Fig. S3 (A), the diffraction peaks intensity of CSNS x nm samples are obviously increased along with the S^{2-}/Cd^{2+} precursor ratios increasing from 1:2 to 3:2, however, the enhancement peaks intensity trend of the Ni_3S_2 species are stronger than that of CdS. Moreover, comparing from Fig. S3 (B), (C) and (D), it also can be found that , (i) the peaks positions of Ni 2p for all the CSNS samples shift to lower banding energy tendency compared with that in pure Ni_3S_2 (Fig. S3B), (ii) while the Cd 3d peaks in CSNS samples shift to higher values than that of pure CdS (Fig. S3C), and (iii) the S 2p energy peaks of CSNS samples locate between at that of pure CdS and pure Ni_3S_2 (Fig. S3D). These banding energy shifts of CSNS samples indicate that some Ni atoms

insert into the CdS crystal cell. This results further confirm the intimate coupling between CdS and Ni_3S_2 for the CSNS samples.

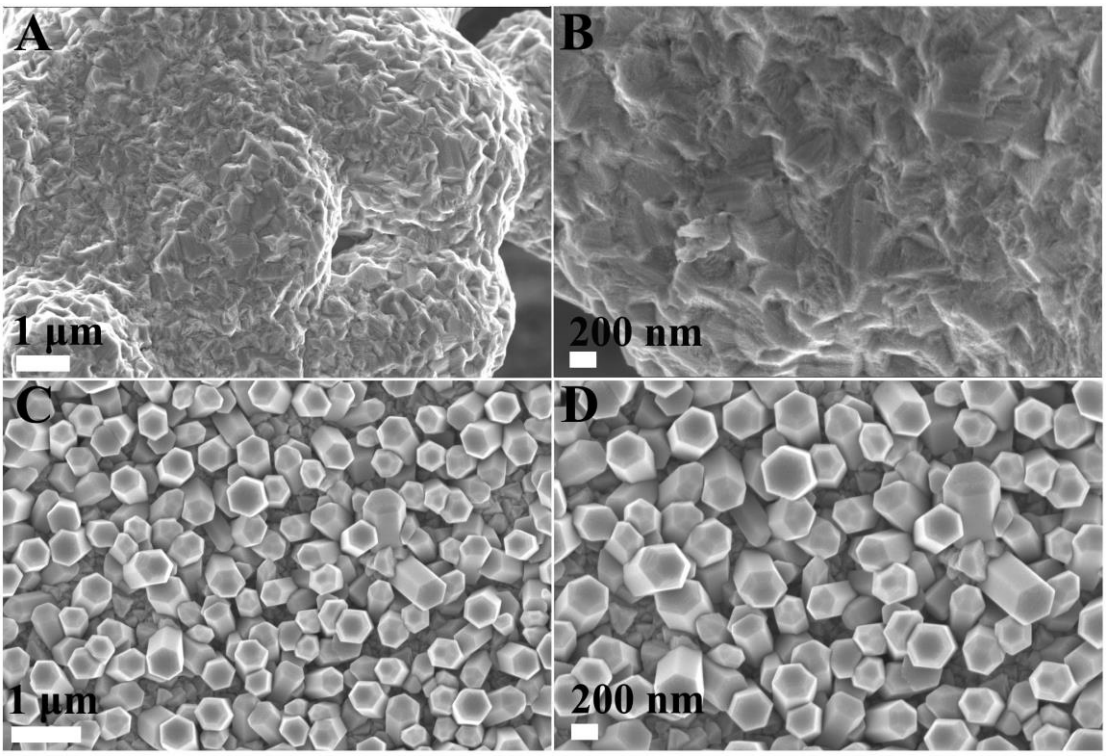

Fig. S4. SEM imagens of pure Ni_3S_2 (A and B) and CdS nanorod arrays (C and D).

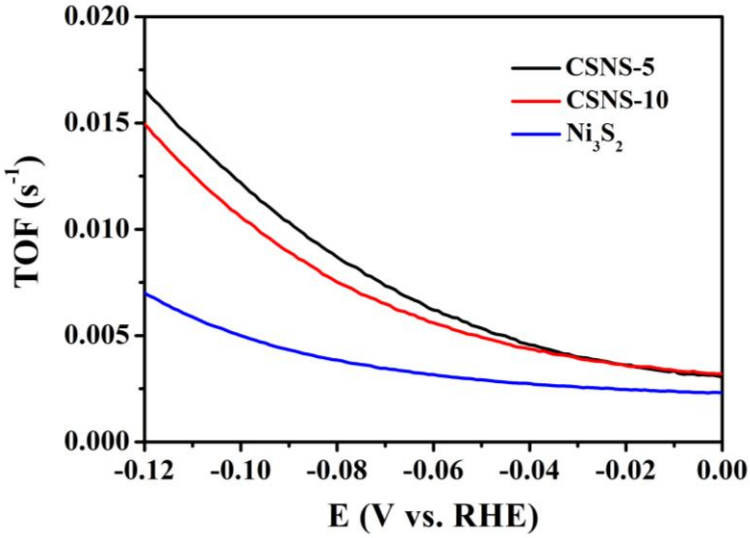

Fig. S5. TOFs of CSNS-5, CSNS-10 and pure Ni_3S_2 samples calculated at various potentials for HER electrocatalysis.

The calculation of turnover frequencies (TOFs) in Fig. S5

According to previous report,[1] the TOFs of the CSNS-5, CSNS-10 and pure Ni_3S_2 were derived from the following equation (S1):

$$\mathrm{TOF}(S^{-1}) = [i \times \frac{1H_2}{2e^-} \times 1\frac{e^-}{q_e}]/N_{active} \quad \text{(S1)}$$

Where, the current (i) was experimentally determined from the electrochemical measurement, and q_e is the electron charge of 1.602×10^{-19} C, N_{active} is the number of active surface atoms. In this work, the N_{active} was determined using the ECSA (Fig. S9 and Table. S1), as described in the following equation (S2)

$$N_{active} = ECSA(cm^2) \times N_{aso}(atoms/cm^2) \quad \text{(S2)}$$

the N_{aso} refer to the surface occupancy of catalytic active substances on the electrode surface, which was calculated by previous reported method using the average atoms in the molar volume to a surface.[2] This approach provide a crude upper bound for the TOF values. As following the molar volume (V_m) of Ni_3S_2 is calculated to be:

$$V_m = \frac{F_w}{\rho} = \frac{240.4\ (g/mol)}{5.89\ (g/cm^3)} = 40.783(cm^3/mol)$$

therefore, the N_{aso} is:

$$N_{aso} = [\frac{1}{V_m} \times \frac{5\times6.02\times10^{23}(\text{atoms})}{1\ (\text{mol})}]^{\frac{2}{3}} = 1.57\times 10^{15}(\text{atoms/cm}^2)$$

Finally, Nactive were calculated by integrating Naso into the equation (2), and then the TOFs can be obtained from equation (1).

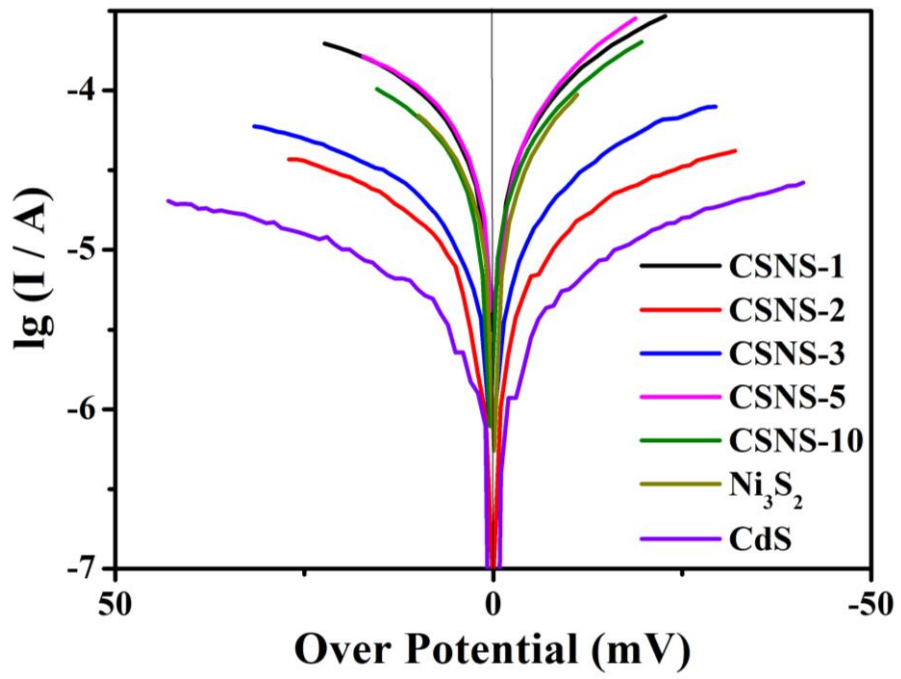

Fig. S6 Tafel plot of all the synthesized samples.

In Fig. S6, the Tafel plot of all the synthesized samples were measured by using electrochemical test, then according to the simplified Butler-Volmer equation (S3)

$$j_k = j_0(e^{\frac{\alpha F}{RT}\eta} - e^{\frac{-(1-\alpha)F}{RT}\eta}) \quad \text{(S3)}$$

where F, R, and T have their usual significance, j_k and j_o stand for kinetic and exchange current density, respectively, the exchange current density (j_0) for all the synthesized samples were obtain as shown Table S1,[3]

Table S1. Calculated exchange current density for all the synthesized samples.

Samples	CSNS-1	CSNS-2	CSNS-3	CSNS-5	CSNS-10	Ni_3S_2	CdS
Log (j_0)	-4.184	-4.996	-4.819	-4.298	-4.478	-4.554	-5.242
j_0 (mA)	0.065	0.010	0.015	0.050	0.033	0.028	0.006

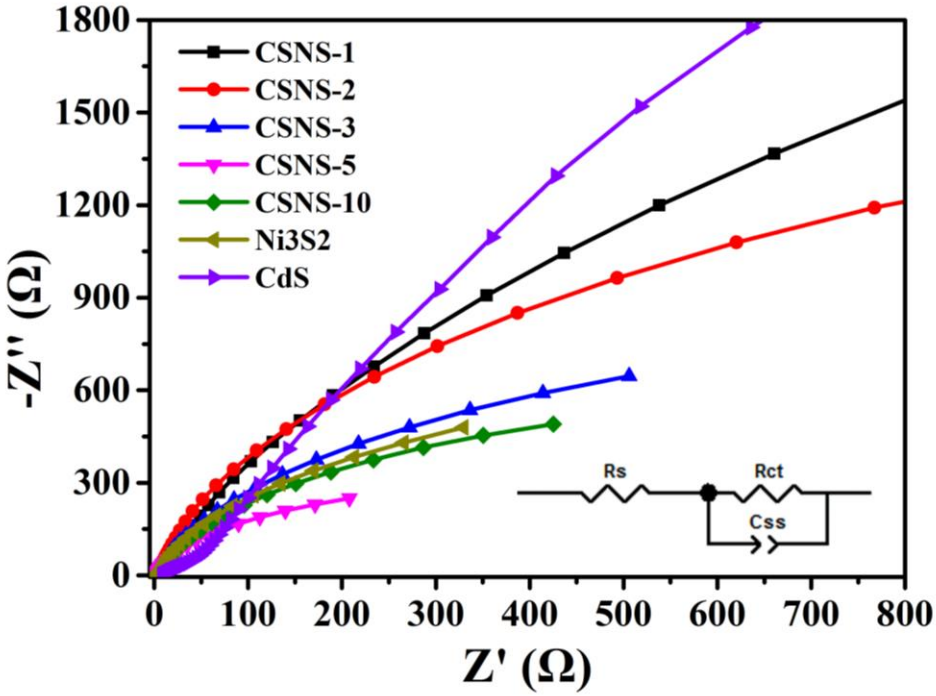

Fig. S7. Nyquist plots of all the CSNS-x samples, pure CdS and Ni_3S_2.

As can be seen in the EIS plot, the equivalent circuit (inset in Fig. S7) is composed of three electrochemical parameters, R_s, R_{ct} and CPE, which represent the electrolyte resistance, charge-transfer resistance and a constant phase element, respectively. Obviously, it is found that the R_{ct} values are gradually decreased from CSNS-1 to CSNS-5, this result indicates that the increased Ni_3S_2 amounts enhance the electronic conductivity of the synthesized electrodes. While, the CSNS-10 electrodes exhibit a similar R_{ct} value as that of pure Ni_3S_2 electrodes, which are a little higher than that of CSNS-5. This phenomenon may be caused by the diffusion effect of electrolyte solution on the electrode surface as the ECSA value of CSNS-5 is higher than that of these two samples.

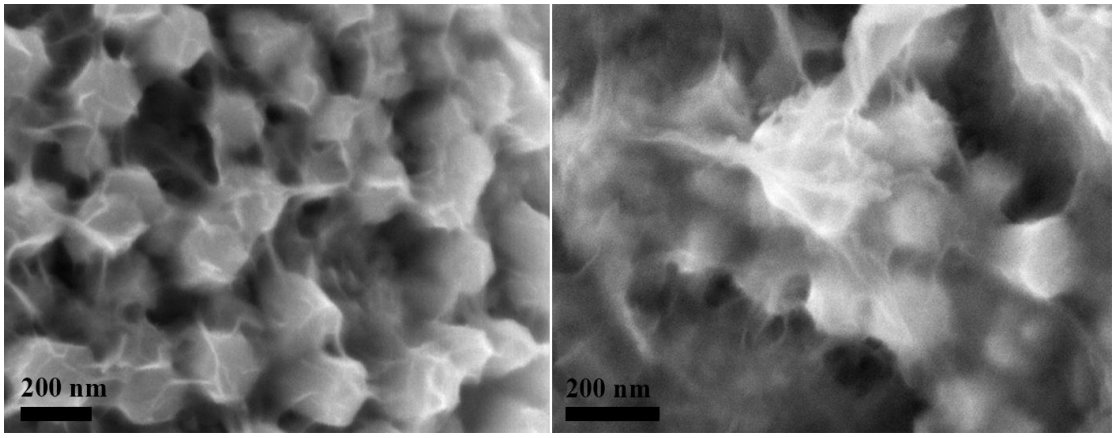

Fig. S8. High magnification SEM images of CSNS-10 core@shell nanorods arrays.

The Fig. S8 reveals the high magnification SEM images of CSNS-10 with a thick Ni_3S_2 nanosheets layers. It can be seen from Fig. S5 A that the Ni_3S_2 nanosheets on different nanorods have combined with each other into a whole layer covering on the surface of CdS nanorods. And in this sample, we have also found that some Ni_3S_2 nanosheets have fully covered the spaces between the nanorods with a relative flat surface. This result would largely reduce the catalytic active sites due to the decreased exposing surface of Ni_3S_2 nanosheets.

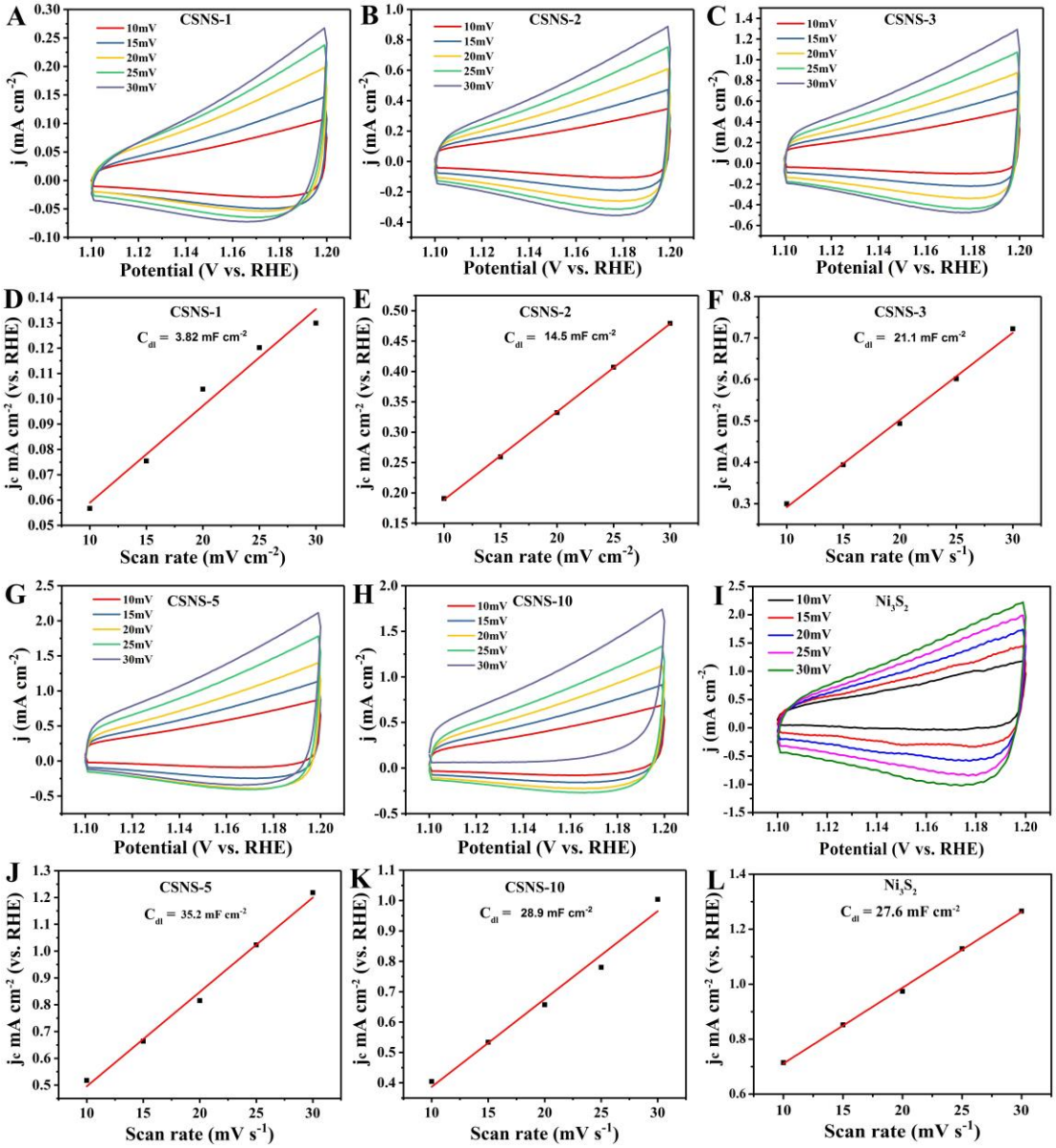

Fig. S9. (A-E) CV cures of CSNS-x samples under various scan rates from 10 to 30 mV s^{-1} in the non-Faradaic potential range (1.1 ~ 1.2 eV vs Ag/AgCl); (F-J) the corresponding C_{dl} plot of CSNS-x samples derived from current densities at 1.15 V vs RHE (in A-E) against the scan rates, and (A, E) for CSNS 1 nm; (B, G) for CSNS-2; (C, H) for CSNS-3; (D, I) for CSNS-5; (E, J) for CSNS-10, respectively.

According to the Fig. S9, the calculated ECSA values for CSNS-x samples were summarized in the following Table S2.

Table S2. Comparison of ECSA towards the different CSNS-x catalysts

Sample	C_{dl} (mF cm^{-2})	ECSA (cm^2)
CSNS-1	3.82	95.5
CSNS-2	14.5	362.5
CSNS-3	21.1	527.5
CSNS-5	35.2	880
CSNS-10	28.9	722.5
Ni_3S_2	27.6	690.0

Table S3

Summary of electrochemical data of Partial Ni based electrocatalysts

Electronic catalysts	Working solution	OER			HER			Reference
		On set potential (V vs. RHE)	η to 20 mA cm^{-2} (mV)	Tafel lope (mV dec^{-1})	On set potential (V vs. RHE)	η to 10 mA cm^{-2} (mV)	Tafel slope (mV dec^{-1})	
CdS@Ni_3S_2-5	**1.0M KOH**	**1.49**	**310**	**176.8**	**-0.03**	**142**	**138.6**	**This work**
CuO@Ni-P NA/CF	1.0M KOH	ab. 1.5	--	124.9	ab. -0.03	ab. 95	72.0	4
Ni-P/CF		Ab 1.6	--	--	ab. -0.14	ab. 200	--	
Ni_3Te_2 (Electrodeposition)	1M KOH	1.38	Ab 200	54.2	Ab. -0.2	250	73.1	5
Ni_3Te_2 (Hydrothermal)		1.38	Ab 220	61.5	Ab. -0.1	250	126.2	
Ni_3S_2/NF	1M KOH	Ab. 1.33	ab. 270	--	Ab. -0.14	Ab. 290	--	6
	PBS(pH=7)	--	--	--	Ab. -0.05	Ab. 150	--	
Fe-$Ni(OH)_2$/NF	1M KOH	Ab. 1.48	Ab. 280	51.5	--	--	--	7
Zn-Ni_3S_2/NF	1M KOH	Ab. 1.51	--	87	--	--	--	8
MoO_3/Ni_3S_2/NF	1M KOH	--	--	--	Ab. -0.1	Ab. 180	--	9
CdS-MoO_3/Ni_3S_2/NF		--	--	--	Ab. -0.03	Ab. 90	--	
Ni_3S_2/PNF	1M KOH	Ab. 1.47	Ab. 290	238	Ab. -0.1	Ab. 220	118	10
1mM CdS/Ni_3S_2/PNF		Ab. 1.5	Ab. 350	192	Ab. -0.1	Ab. 180	110	
3mM CdS/Ni_3S_2/PNF		--	--	--	Ab. -0.1	Ab. 220	187	
5mM CdS/Ni_3S_2/PNF		--	--	--	Ab. -0.1	Ab. 220	167	
Ni_2P nanowires	1M KOH	Ab. 1.51	Ab. 340	47	--	--	--	11
Ni_2P nanoparticles		Ab. 1.47	Ab. 300	59	--	--	--	
$Ni(OH)_2$		Ab. 1.51	Ab. 340	59	--	--	--	
Ni_3Se@Au(No dissolution)		1.43	Ab. 330	87.1	-0.19	Ab. 380	188.1	12

Ni_3Se@Au(15s dissolution	1M NaOH	1.40	Ab. 270	54.6	-0.16	Ab. 320	234.4	
Ni_3Se@Au(30s dissolution)		1.39	Ab. 260	48.9	-0.16	Ab. 310	230.4	
Ni_2P-NRs/Ni	0.5M H2SO4	--	--	--	Ab. -0.1	Ab. 180	106.1	13
$Ni(OH)_2$@NF	1M KOH	--	--	--	Ab. -0.05	Ab. 180	107.4	14
Ni_3S_2@NF		--	--	--	Ab. -1.2	Ab. 220	50.2	
MS-Ni_3Se_2/Ni	1M KOH	Ab. 1.60	--	--	Ab. -0.24	Ab. 250	118	15
NF-Ni_3Se_2/Ni		Ab. 1.50	--	--	Ab. -0.16	Ab. 210	79	
NiS-$Ni(OH)_2$/aMoS^{2+}_x	1M KOH	Ab. 1.55	460	97	Ab. -0.12	Ab. 170	81	16
$NiCo_2S_4$/NF	1M KOH	Ab. 1.50	--	53.3	Ab. -0.09	Ab. 220	97.1	17
Ni_3S_2/NF		Ab. 1.55	Ab. 350	103.3	Ab. -0.17	Ab. 300	116.3	
$NiCo_2O_4$/NF		Ab. 1.55	Ab. 330	97.7	Ab. -0.15	Ab. 320	107.5	
Mn-Ni_2P/NF	1M KOH	--	--	--	Ab. -0.13	103	135	18
Ni_2P/NF		--	--	--	Ab. -0.2	82	138	
NiS/NF	1M KOH	Ab. 1.52	--	89	Ab. -0.1	Ab. 180	83	19

Ab. : the estimated data from the correspoding references

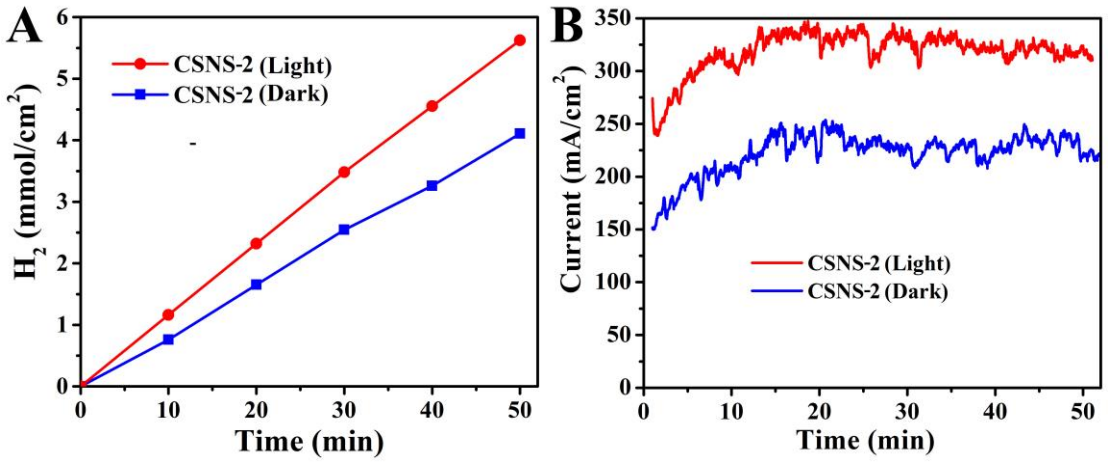

Fig. S10. (A) EC (blue line) and PEC (red line) H_2 evolution properties of CSNS-2 sample under 0.2 V external bias (vs Ag/AgCl) in the Na_2S and Na_2SO_3 mixed solution, and (B) the recorded electrical (blue line) and photo-electrical (red line) current intensity during the EC and PEC H_2 evolution process.

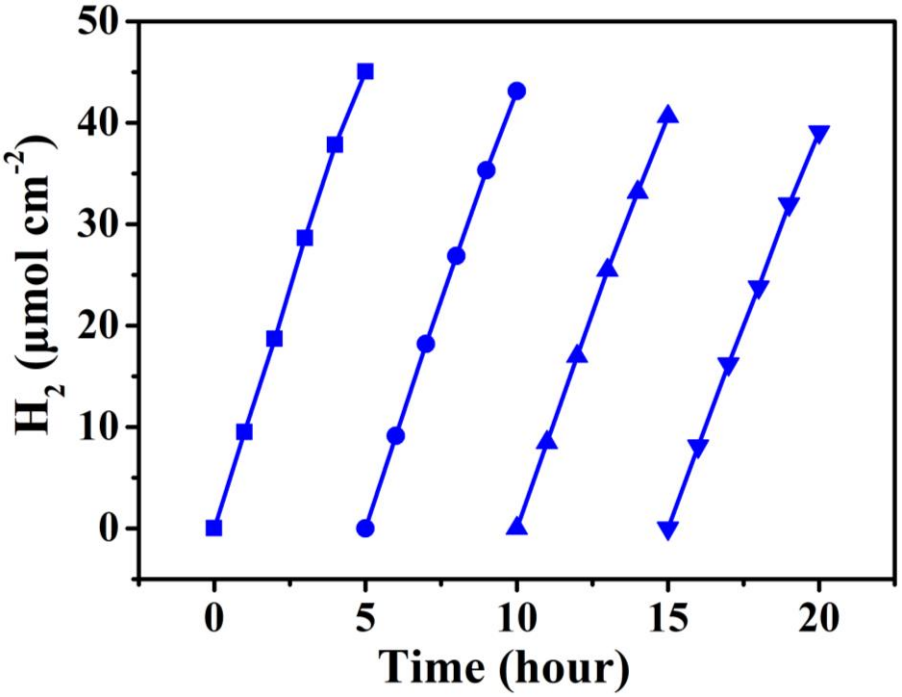

Fig. S11. Time course of photocatalytic H_2-production over CSNS-5 sample, every five hours the reaction system was bubbled with N_2 for 30 min to remove the H_2 inside in the reactor.

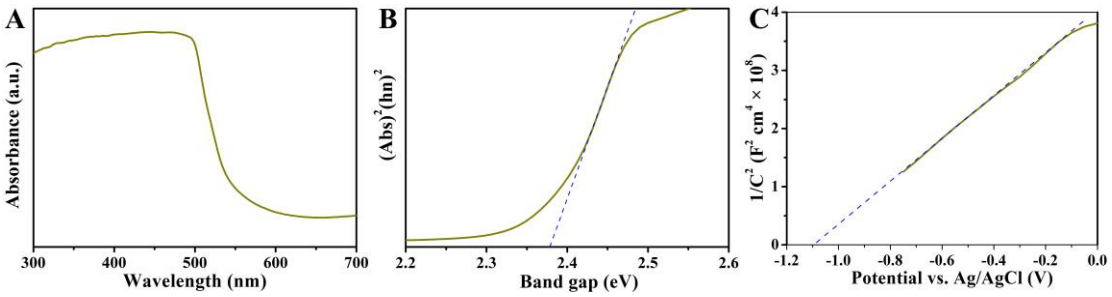

Fig. S12. The UV-visible diffuse reflection spectra (A), the translated Tauc plots and the Mott-Schottky (MS) plots of pure CdS nanorod arrays.

The band gap structure of pure CdS nanorod arrays was measurements by the UV-visible diffuse reflection spectra, the translated Tauc plots and the Mott-Schottky plots as shown in Fig. S12. According to the UV-visible diffuse reflection spectra (A), the band gap of CdS nanorod arrays were determined to be 2.38 eV (B), and the Mott-Schottky (MS) plots reflected that the E_{fb} of CdS is about -1.10 eV. Therefore, the CB and VB position of CdS was estimated to be at -1.30 and 1.08 eV (vs Ag/AgCl), respectively.

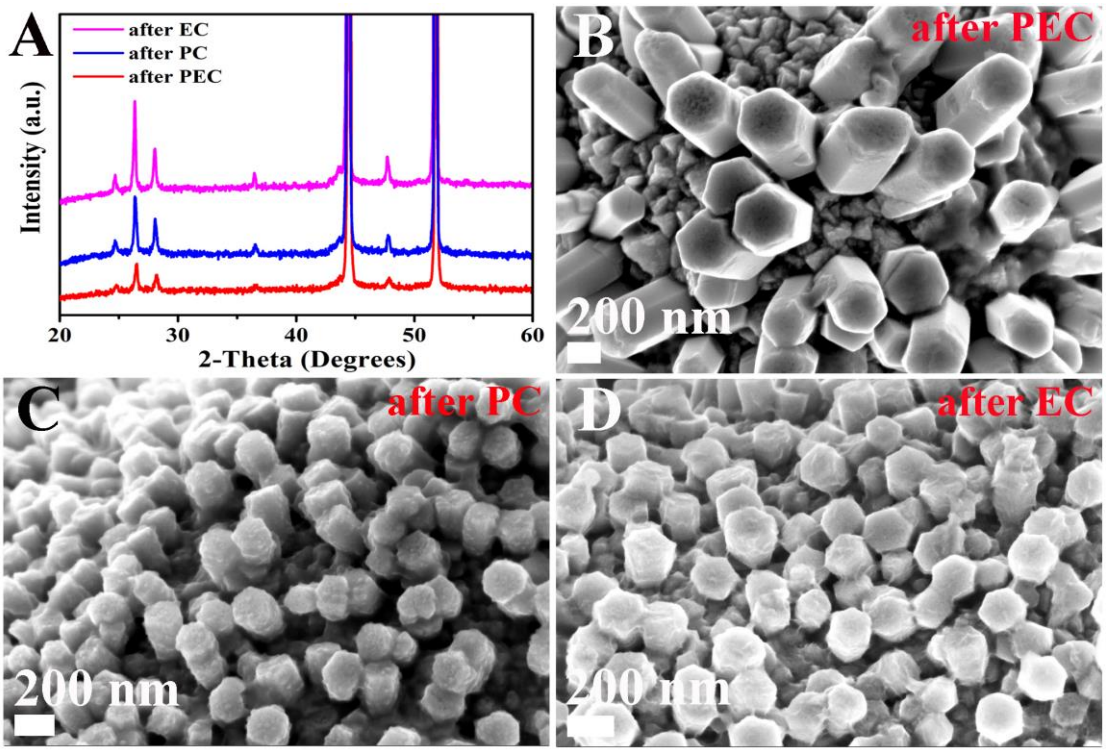

Fig. S13. The XRD patterns (A) and corresponding SEM imagens of CSNS-2 (B), CSNS-3 (C) and CSNS-5 (D) after the long time PEC, PC and EC process.

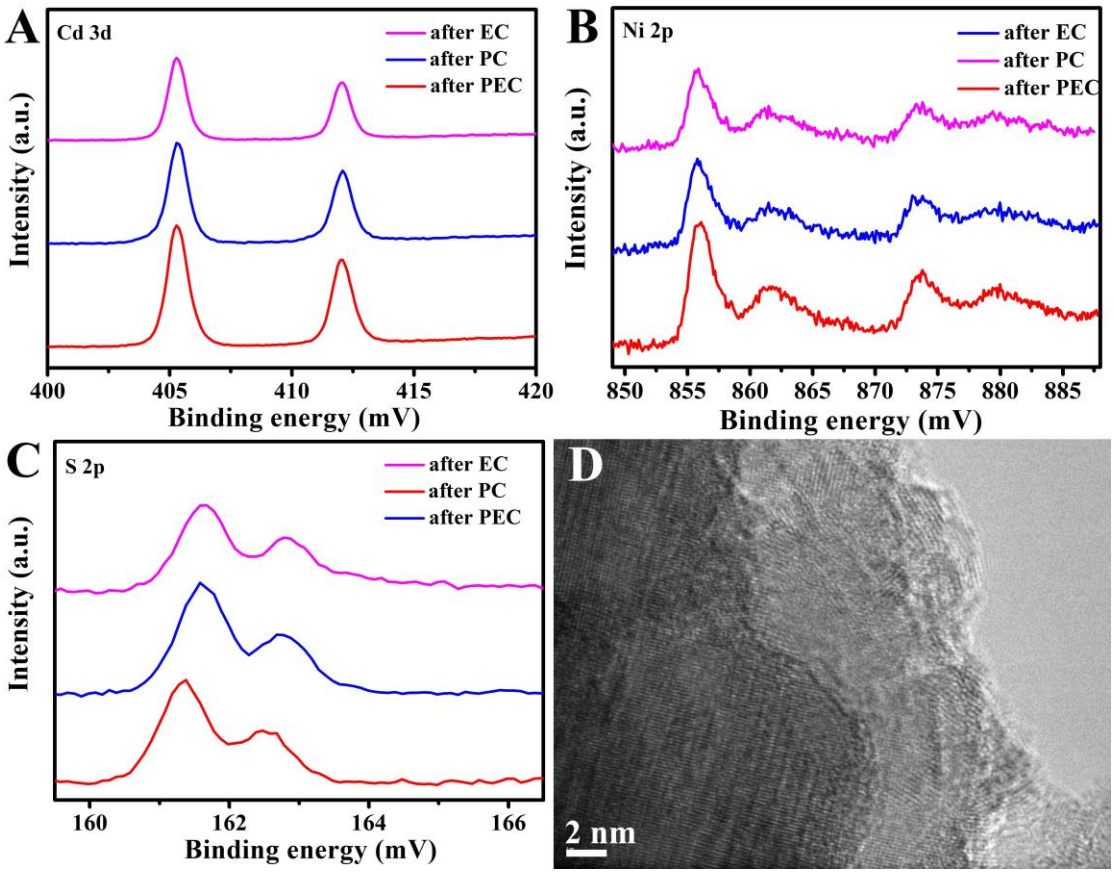

Fig. S14. XPS spectra of Cd 3d (A), Ni 2p (B) and S 2p (C) for CSNS-2, CSNS-3 and CSNS-5 after the long time PEC, PC and EC process.. The results indicate that the surface structure remained unchanged after corresponding catalysis process.

References

1. B. Seo, D. S. Baek, Y. J. Sa and S. H. Joo, *CrystEngComm*, 2016, **18**, 6083-6089.
2. E. J. Popczun, J. R. McKone, C. G. Read, A. J. Biacchi, A. M. Wiltrout, N. S. Lewis and R. E. Schaak, *J. Am. Chem. Soc.*, 2013, **135**, 9267-9270.
3. A. Oh, Y. J. Sa, H. Hwang, H. Baik, J. Kim, B. Kim, S. H. Joo and K. Lee, *Nanoscale*, 2016, **8**, 16379-16386.
4. B. Chang, S. Hao, Z. Ye and Y. Yang, *Chem. Commun*, 2018, **54**, 2393-2396.
5. U. De Silva, J. Masud, N. Zhang, Y. Hong, W. P. R. Liyanage, M. Asle Zaeem and M. Nath, *J. Mater. Chem. A*, **2018,** *6*, 7608-7622.
6. L. L. Feng, G. Yu, Y. Wu, G. D. Li, H. Li, Y. Sun, T. Asefa, W. Chen and X. Zou, *J. Am. Chem. Soc.*, **2015,** *137*, 14023-6.

7. J. Liu, Y. Zheng, Z. Wang, Z. Lu, A. Vasileff and S. Z. Qiao, *Chem. Commun.*, **2018,** *54*, 463-466.
8. Q. Liu, L. Xie, Z. Liu, G. Du, A. M. Asiri and X. Sun, *Chem. Commun.*, **2017,** *53*, 12446-12449.
9. W. Lu, Y. Song, M. Dou, J. Ji and F. Wang, *Chem. Commun.*, **2018,** *54*, 646-649.
10. S. Qu, J. Huang, J. Yu, G. Chen, W. Hu, M. Yin, R. Zhang, S. Chu and C. Li, *ACS Appl. Mater. Interfaces*, **2017,** *9*, 29660-29668.
11. L. A. Stern, L. G. Feng, F. Song and X. L. Hu, *Energy Environ. Sci.*, **2015,** *8*, 2347-2351.
12. A. T. Swesi, J. Masud and M. Nath, *J. Mater. Res.*, **2016,** *31*, 2888-2896.
13. X. Wang, Y. V. Kolen'ko and L. Liu, *Chem. Commun.*, **2015,** *51*, 6738-41.
14. M. Wu, S. Wang and J. Wang, *Electrochim. Acta*, **2017,** *258* , 669-676.
15. R. Xu, R. Wu, Y. Shi, J. Zhang and B. Zhang, *Nano Energy*, **2016 ,** *24*, 103-110.
16. T. Yoon and K. S. Kim, *Adv. Funct. Mater.*, **2016,** *26*, 7386-7393.
17. J. Yu, C. X. Lv, L. Zhao, L. X. Zhang, Z. H. Wang and Q. Y. Liu, *Adv. Mater. Interfaces*, **2018,** *5*, 1701396.
18. Y. Zhang, Y. Liu, M. Ma, X. Ren, Z. Liu, G. Du, A. M. Asiri and X. Sun, *Chem. Commun.*, **2017,** *53*, 11048-11051.
19. W. Zhu, X. Yue, W. Zhang, S. Yu, Y. Zhang, J. Wang and J. Wang, *Chem. Commun.*, **2016,** *52* , 1486-9.